Icarus 209 (2010) 262–270

Contents lists available at ScienceDirect

Icarus

journal homepage: www.elsevier.com/locate/icarus

Evaluation of the origin hypotheses of Pantheon Fossae, central Caloris basin, Mercury

Christian Klimczak *, Richard A. Schultz, Amanda L. Nahm [1]

Geomechanics – Rock Fracture Group, Department of Geological Sciences and Engineering, MS172, University of Nevada, Reno, NV 89557, USA

ARTICLE INFO

Article history:
Received 24 October 2009
Revised 16 April 2010
Accepted 20 April 2010
Available online 24 April 2010

Keywords:
Mercury
Tectonics

ABSTRACT

The origin of Pantheon Fossae, a complex structure consisting of radial graben in the center of the Caloris basin, Mercury, has been debated since the structure was first imaged by the MESSENGER spacecraft. Three different formation hypotheses have been suggested, i.e. an origin associated with the Apollodorus impact into a previously domed Caloris basin floor, graben formation as surface expressions of dike intrusions and basin-interior uplift alone. In order to test the scenarios, detailed observations from the currently available imagery were compared to the proposed formation mechanisms. We evaluate these origin hypotheses by means of detailed interpretations of the graben characteristics and patterns, by comparing to radial structures from Earth and Venus, and by mechanical analyses for each formation hypothesis. Results indicate that the formation of Pantheon Fossae as the result of doming in the central part of the Caloris basin is more likely than it having formed in association with a radially symmetric stress field centered at or near the Apollodorus crater, that would have been created by a magma chamber or been superimposed on a pre-existing dome due to impact mechanics.

© 2010 Elsevier Inc. All rights reserved.

1. Introduction

During its first flyby in 2008, the Mercury Surface, Space Environment, Geochemistry and Ranging (MESSENGER) spacecraft revealed previously unseen parts of Mercury's surface, among which was Pantheon Fossae (Fig. 1a). Pantheon Fossae constitutes an array of ~230 radial graben that occur near the center of the ~1500 km diameter Caloris impact basin. Near the center of Pantheon Fossae is the 40 km diameter Apollodorus impact crater and its surrounding ejecta blanket (Murchie et al., 2008) (Fig. 1a). The majority of the graben occur within a radius of 175 km from the central region of Pantheon Fossae; however, a few graben extend further into the outer Caloris basin, where they connect with radial and circumferential troughs, creating a large scale polygonal pattern (Watters et al., 2009b; Watters and Nimmo, 2009).

Extensional deformation on Mercury is rare, with a prominent example observed as circumferential graben and the polygonal pattern of troughs in the Caloris basin. Pantheon Fossae is, so far, the only example of its kind observed on Mercury. Among all discoveries made by MESSENGER, Pantheon Fossae's status is considered special (Head et al., 2009; Freed et al., 2009; Watters et al., 2009a,b; Watters and Nimmo, 2009), since it will help to further characterize the deformation history of the Caloris basin. Plausible explanations for the formation of the radial pattern of the graben will therefore lead to better insights into the post-impact evolution and deformation in and around the Caloris basin.

2. Characteristics of the graben of Pantheon Fossae

The majority of the ~230 radial graben of Pantheon Fossae, located in the central Caloris basin, are developed within ~175 km from their convergence point. Previous studies described some general characteristics of the radial graben, where it was noted that graben lengths range from 5 km to 110 km and graben widths range from 1 km to 8 km (Murchie et al., 2008; Watters et al., 2009b; Head et al., 2009). Several other important characteristics can be obtained from the MESSENGER imagery, permitting, for the first time, a quantitative evaluation of the proposed formation hypotheses (Fig. 1).

Two sets of graben can be distinguished by their different widths and orientations (Fig. 1a). Graben of set 1 (Fig. 1a, outlined in black) have narrow widths ranging between 1 km and 2.5 km. Graben of smaller widths are currently not resolved. Set 1 graben are all, without exception, oriented radial to a central point. This set contains the most graben and continues outward radially as much as 230 km from their point of convergence. Graben of set 2 (Fig. 1a, outlined in white) differ from set 1 graben in width, orientation, geographic occurrence, and number. There are only 4–5 individual graben in this set, which have widths of up to 8 km.

* Corresponding author. Fax: +1 775 784 1833.
E-mail address: klimczak@unr.nevada.edu (C. Klimczak).
[1] Present address: Center for Lunar Science and Exploration, USRA – Lunar and Planetary Institute, 3600 Bay Area Blvd., Houston, TX 77058, USA.

0019-1035/$ - see front matter © 2010 Elsevier Inc. All rights reserved.
doi:10.1016/j.icarus.2010.04.014

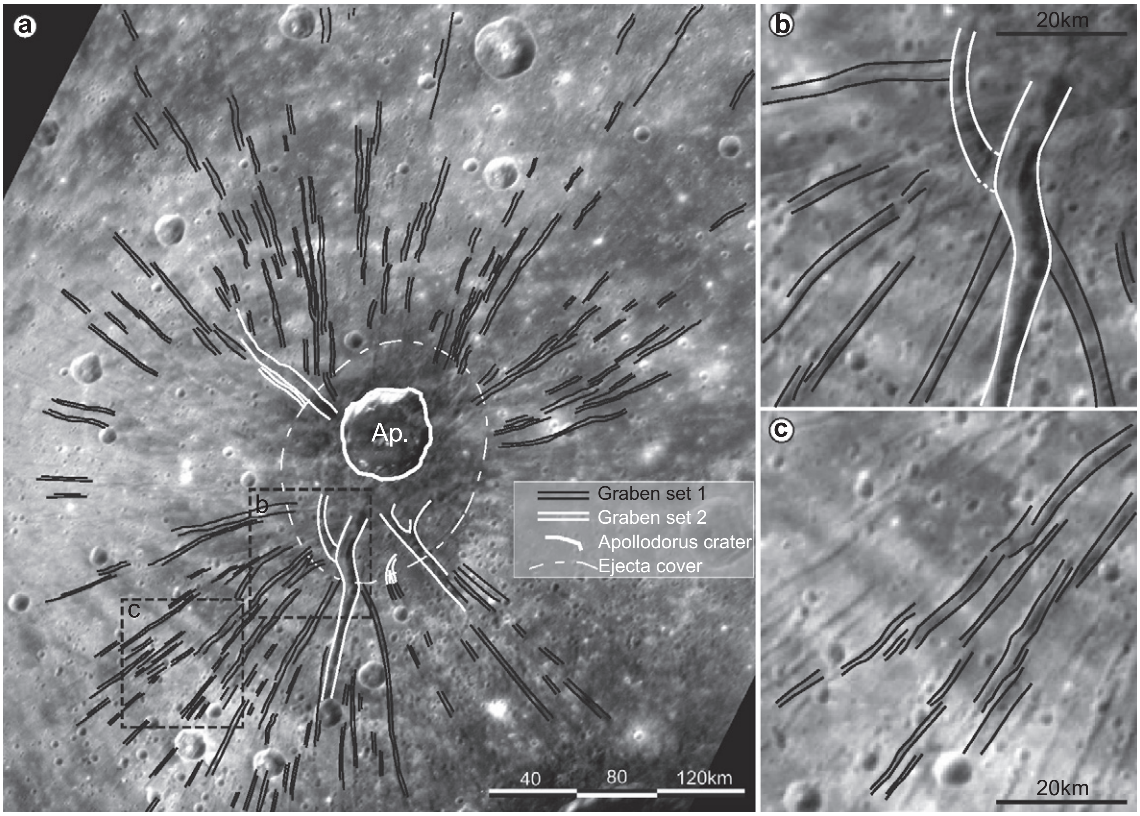

Fig. 1. MESSENGER image mosaic of Pantheon Fossae, Mercury. Planetary data system images (CN0108826757M and CN0108826822M) taken by the Mercury Dual Imaging System Narrow Angle Camera have a spatial resolution of ~280 m per pixel. (a) Map of Pantheon Fossae showing two sequential sets of graben identified in this study. Set 1 graben (black) includes numerous narrow graben, whereas graben of set 2 (shown in white) include fewer but significantly wider graben. Graben are covered around their radially projected point of convergence by the Apollodorus impact (thick white line) crater and its surrounding ejecta blanket (outermost extent approximated by dashed white line). (b) Close-up image of set 2 graben (white) cross-cutting graben of set 1 (black). (c) Neighboring graben of set 1 display right and left step-over geometries.

They have different orientations with respect to graben of set 1, and occur only close to the central part of Pantheon Fossae and radiate no more than 120 km outward. The orientations of set 2 graben progressively assume the orientations of set 1 graben with increasing distance from the point of convergence. In the central part of Pantheon Fossae, set 2 graben clearly cross-cut graben of set 1 (Fig. 1b). This cross-cutting relationship allows the determination of the age relationship between the two sets of graben, with the graben of set 2 being consistently younger than set 1.

Ejecta from the Apollodorus impact covers the innermost parts of the graben of set 1 and to an extent also graben of set 2 (Fig. 1a). Furthermore, graben of set 1 show left and right step-over geometries (Fig. 1c), also referred to as relay ramps (e.g., Peacock and Sanderson, 1991). This is indicative of normal faulting (e.g., Peacock, 2002; Schultz et al., 2007) and confirms that these troughs are indeed graben. Most of the Pantheon Fossae graben have widths that do not vary along their lengths, remaining relatively constant throughout the length of each graben (Fig. 1a).

The width of a graben can be used to estimate the depth of faulting (DOF) according to the "hourglass" model first used and applied to the graben of Canyonlands National Park, Utah (Schultz et al., 2007). Utilizing the optimum orientation of the frictional slip plane θ_{opt} (Jaeger and Cook, 1979) of the normal faults and the widths of the graben, the DOF for the faults of the graben can be determined. We use an optimum orientation of the frictional slip plane of $\theta_{opt} = 61.5°$, consistent with an internal friction coefficient of 0.65 for basalt (Byerlee, 1978). By comparison, Watters et al. (2009b) used a comparable fault plane dip angle of $\theta_{opt} = 60°$ for strain calculations of the Caloris graben. The difference in these values does not contribute to a significant difference in depth of graben faulting, given the uncertainties in measurements of graben widths in the MESSENGER imagery.

A total of 157 graben in the Pantheon Fossae array have been analyzed in terms of the DOF of their bounding normal faults. DOF is shown in Fig. 2 as a function of the radial distance of the center of the graben away from their common point of convergence. It is apparent that there are two main DOF values for the faults bounding the graben. The two DOF values relate to the two sets of graben, with the set 1 graben having a DOF of approximately 3 km, whereas faults of the second set of graben have DOFs up to 13 km. These DOFs along with constant along-strike graben widths indicate that the faults might be vertically restricted to two successive stratigraphic or mechanical units (e.g., Nicol et al., 1996; Polit et al., 2009) within the Caloris basin.

In order to explore the radial variation of fault-related strain with distance from their center of convergence, we calculated the circumferential strain accommodated by the graben of Pantheon Fossae along six uniformly spaced circular traverses (Fig. 3). Strain calculations are based on measurements of shadows of graben walls onto the graben floor, since there is no independent topographic information currently available for these structures. With known incidence angle of the Sun and a given orientation of the fault planes, shadow length measurements allow determination of the magnitude of extension accommodated by the normal faulting. Incidence angles of the Sun were obtained from the header files of the used MESSENGER image data. Accurate measurements of 23 shadows were made, given that these shadows are only wide enough to be resolved at the graben that were oriented more or less perpendicular to the azimuth angle of the Sun. Most other graben were too narrow to enable accurate shadow length measure-

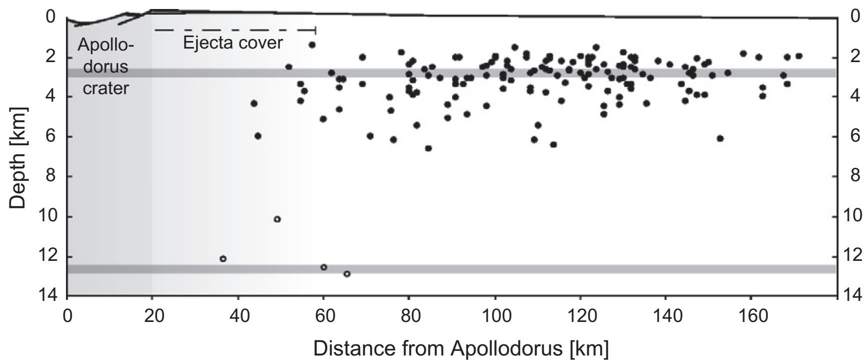

Fig. 2. Calculated depth of faulting (DOF) is shown for every analyzed graben with distance away from the center of convergence. DOF for set 1 graben (filled dots) and set 2 graben (open dots) indicated by bold gray lines at ~3 km and at ~13 km, respectively. Locations of Apollodorus crater and ejecta blanket are shown as reference.

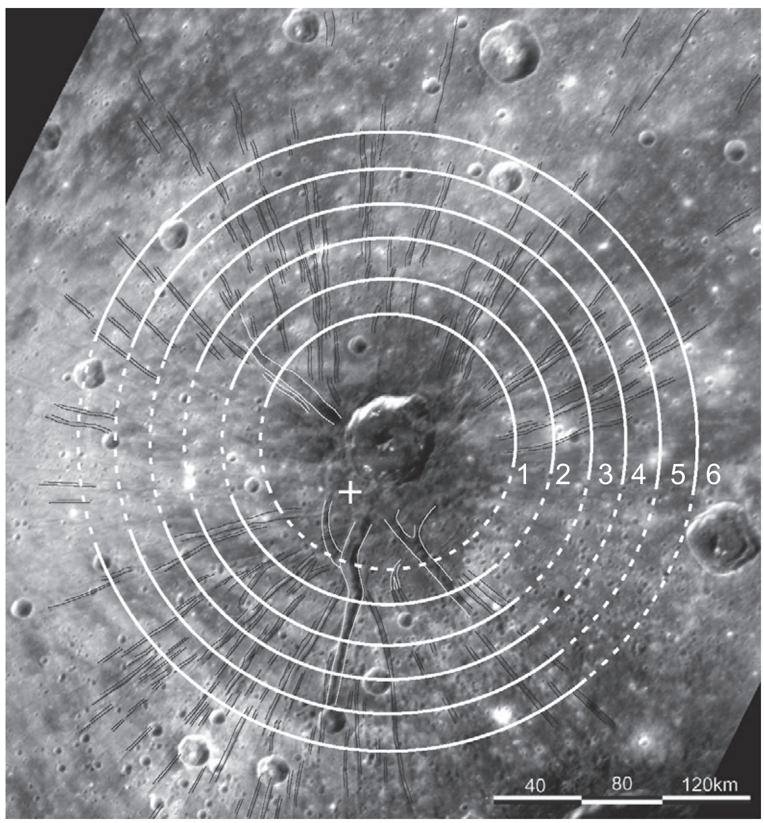

Fig. 3. Location of the six traverses used for the Apollodorus hypothesis evaluation, along which the circumferential strain was determined. The white cross southeastward of Apollodorus crater indicates the true geometric center of radial convergence of all graben, which was used as a center for the concentric traverses to determine strain for dike emplacement and uplift evaluations.

ments to be made, since the topography of these graben is not pronounced enough in order for their shadows to be wide enough to be definitively resolved on the imagery. These measurements were then compared to the graben widths, which revealed a linear relationship between shadow lengths and graben widths. This relationship was used to extrapolate shadow measurements to all analyzed graben and the circumferential strain was computed along the six traverses. The values of the strain calculations provide accurate estimates for the Pantheon Fossae graben structure, since any smaller faults of the population, unresolved in the available imagery, would contribute a negligibly small amount to the total fault-related strain (e.g. Scholz, 2002).

Results of the extensional strain calculations yield fairly consistent values throughout the six traverses of ~1.5–3% of extension, where the highest strain values of ~3.5% were obtained along traverses two and three, which then consistently fall off towards traverse six to values of 1.5%. Compared to areal extensional strain calculations from Watters et al. (2009b) for the entire Caloris basin, where values of ~0.02–0.13% were obtained, our results show an increased extensional strain in the Caloris basin center. Interestingly, the strain accommodated by the Pantheon Fossae graben structure is relatively constant, with no significant or monotonic increase or decrease with radial distance from the geometric center of the fault sets. In addition to the radial fault geometry, multi-stage history, and consistent depths of faulting referred to above, these values of circumferential extensional strain provide a quantitative description of the degree and pattern of extension that any geodynamic model for the Caloris basin must match for a successful prediction of Pantheon Fossae faulting to be achieved.

In the following sections, we use our observations to evaluate and test each of the proposed origin hypotheses for the formation of Pantheon Fossae. The hypotheses are assessed here based on detailed mapping of the radial graben, interpretations of the mapped patterns, and comparisons of calculated strain with expected strains for each of the proposed origin hypotheses.

3. Previous work and hypotheses

Since its discovery, the origin of Pantheon Fossae has been a matter of debate, and three main origin hypotheses formation have been proposed. These hypotheses suggest that Pantheon Fossae formed in conjunction with the Apollodorus crater-forming impact within an extensional stress field (Freed et al., 2009), are surface expressions of dikes at depth (Head et al., 2008, 2009), or in association with basin-interior uplift alone (Murchie et al., 2008).

The most detailed scenario for the formation of the radial graben has been proposed by Freed et al. (2009). They associated the graben structure with the Apollodorus impact, which is located in the central area of Pantheon Fossae, near the point where all graben converge. This spatial relationship caused Freed et al. (2009) to investigate whether the Apollodorus impact itself induced a sudden stress change in a pre-existing extensional stress state of the Caloris basin center that led to the graben faulting. The pre-existing extensional stress state was created by prior uplift of the Caloris basin floor. They use a series of three-dimensional (3D) finite element models, where stress changes in the central Caloris basin floor materials are modeled as functions of the extent of an impact damage zone in combination with basin uplift, elastic moduli of basin fill and crust material and variations of lithospheric thickness. Based on their calculations, they concluded that, despite most key parameters being unknown, the graben of Pantheon Fossae could have originated from the Apollodorus impact. In particular, the impact is suggested to have instantaneously changed the stress state, causing fill material to move radially outward, which then caused changes in the circumferential and radial that travelled at seismic wave speeds. Consequently, radial faulting would have occurred at the magnitude of seismic rupture, where both seismic wave and rupture propagation speeds were in excess of several kilometers per second.

In the second hypothesis, the graben were alternatively proposed to be surface expression of igneous dikes at shallow depth radiating outward from a over-pressured magma reservoir beneath the central Caloris basin floor (Head et al., 2008, 2009). Radial graben commonly form due to magmatic processes on other terrestrial bodies at comparable scales of Pantheon Fossae. Over-pressurized magma chambers compensate the pressure imbalances by fracturing the surrounding rock, forming steeply dipping radial dikes. These dikes then propagate radially outward from the magma chamber at shallow depths. Similar structures are frequently observed on Venus and Earth (e.g. Ernst, 2001). Head et al. (2008, 2009) use observations from radial structures on Venus to qualitatively assess possible processes involved in the formation of Pantheon Fossae.

As Murchie et al. (2008) and Watters et al. (2009b) noted in the third origin hypothesis, the discovery of radial extension in the central Caloris basin provides new limiting conditions for pre-existing models suggesting Caloris interior extension and associated uplift due to (1) exterior loading (Melosh and McKinnon, 1988; Kennedy et al., 2008) or (2) lateral crustal flow toward the basin center (Watters et al., 2005). All of these uplift models, proposed prior to Pantheon Fossae's discovery, were based on circumferential extensional deformation at the Caloris basin periphery only. They did not yet incorporate greater circumferential than radial extensional stresses in the basin center as indicated by the radial graben pattern of Pantheon Fossae.

4. Evaluation of the hypotheses and discussion

4.1. Apollodorus hypothesis

Based on numerical modeling and theoretical assumptions, Freed et al. (2009) calculate a stress state within the inner Caloris basin that features a circumferential extensional stress regime there as demanded by the radial graben of Pantheon Fossae. They suggested that Pantheon Fossae is the result of a sudden change in a pre-existing extensional stress state. They concluded that the Apollodorus impact created a radial damage zone in which elastic stresses could not be supported and consequently caused a radial outward movement of the basin floor. Resulting stress changes were then inferred to have travelled with seismic speeds to form the Pantheon Fossae graben.

Following their logic, the predicted stresses beyond the impact crater's damage zone not only travelled at seismic velocities but must also have attenuated with distance beyond the damage zone. In addition, the formation of the impact damage zone is caused by interactions between the expanding refraction and compressive impact shock waves (Rinehart, 1968). Hence the formation of the damage zone occurred rapidly after the Apollodorus impact. As a consequence, the hypothesis of Freed et al. (2009) implies that the rock properties in the damage zone changed within the same time frame and thus the changes in the pre-existing stress field to travel with seismic wave speeds. As demonstrated in the literature, the velocities of impact shock waves (Melosh, 1989), seismic waves, and dynamic rupture propagation (Scholz, 2002) radially attenuate as a function of the inverse squared distance from their origin ($1/r^2$). Accordingly, the radial stress decrease should be reflected in the magnitude of circumferential extensional strain at Pantheon Fossae.

In order to compare circumferential strains calculated for the Pantheon Fossae graben with stress predictions by various attenuation models, we convert the circumferential strain, ε, into normal stress, σ, using

$$\sigma = \varepsilon \cdot E, \tag{1}$$

where E is the Young's modulus of the Caloris floor material (see discussion below). For our analysis, we use $E = 1$ GPa as a representative value, which is appropriate to mafic rocks in the near-surface region (e.g. Schultz, 1995). Given that only the circumferential strains across Pantheon Fossae graben can be assessed, this relationship provides an estimate of the amount of stress necessary to produce the observed extension.

Results are plotted in Fig. 4, where several plausible attenuation functions are plotted against the distance, r, away from the center of Apollodorus impact crater. Stress is shown to attenuate as a standard function for seismic waves (Fig. 4, solid lines) as the inverse squared distance from their point of origin ($1/r^2$) and as a more complicated function for impact shock waves (Fig. 4, dashed lines), where peak stresses decline as a function of $1/r^3$ in excess of 0.1 GPa but then decline as $1/r^{3/2}$ when stresses drop below 0.01 GPa (Melosh, 1989). The initial stresses that formed the damage zone are selected based on maximum shock pressures in vertical impacts after the planar impact approximation (Ahrens and O'Keefe, 1977; Melosh, 1989). Values are chosen for iron and gabbroic impactors on a gabbroic target with a minimum impactor

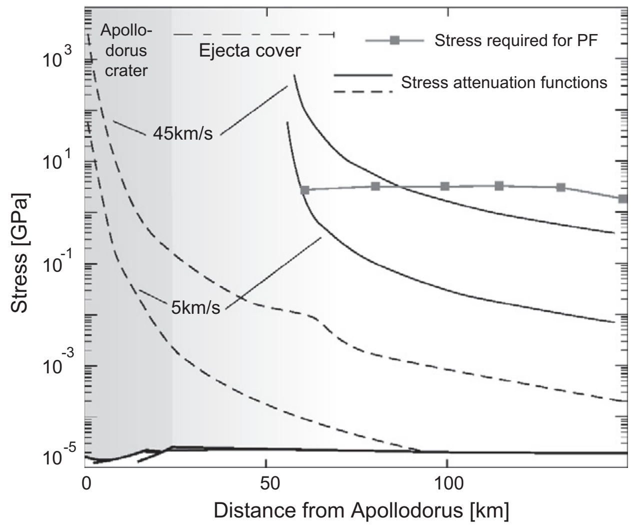

Fig. 4. Calculated attenuation of seismic and impact shock waves as functions of distance from Apollodorus crater in gabbroic material shown in relation to stresses obtained from measured strain that are inferred to form graben of Pantheon Fossae (PF). Solid lines represent stress attenuation as function of the inverse squared distance from the Apollodorus crater with velocities of 45 km/s and 5 km/s. Dashed lines represent more complex attenuation functions for the same velocities. See text for explanation.

velocity of 5 km/s and maximum velocity of 45 km/s, which are likely to bracket that of the Apollodorus impactor.

If the outward movement of Caloris basin fill material or the impact itself caused the graben, the triggered stresses or stress changes from the impact damage zone should be consistent with the strains accommodated by the graben. However, as apparent in Fig. 4, stress values from the impact and related events are substantially different than the stress magnitude inferred from the calculated strain at Pantheon Fossae, since the two stress curves have significantly differing slopes. While the predicted impact-related stresses decrease, the stresses calculated from strain in Eq. (1) related to faulting at Pantheon Fossae are relatively constant and do not show a comparable downward trend with distance from the center of the crater.

The magnitude of the stresses needed to create the graben of Pantheon Fossae depends on the relationship between stress and strain. We choose the simplest one-dimensional (1D) form of Hooke's law (Eq. (1)) since only the circumferential strain is recorded by the graben. Although the values of stress would vary if the radial strain were also included, the geometry of Pantheon Fossae border faults and graben implies a plane-strain environment such that radial strain would be negligibly small (e.g. Krantz, 1989). Hence, stresses are closely related to the chosen Young's modulus. As mentioned above, we use 1 GPa as a representative value for Young's modulus. By choosing a different value of Young's modulus, the magnitude of stress within the damage zone decreases by perhaps a factor of 2–3, but the slope of the curve remains unchanged. Similarly, different values of the initial stresses will not change the slope of the attenuation curves in Fig. 4. Here, the functions would shift along the y-axis, but only slightly.

The magnitude of in situ stresses in the upper kilometers at Pantheon Fossae can be estimated by using $\sigma_v = \rho g z$, where σ_v is the vertical overburden stress, ρ is average crustal density, g is gravity, and z is depth below the surface. Assuming values of $\rho = 3300\ \mathrm{kg/m^3}$ and $g = 3.78\ \mathrm{m/s^2}$ and noting that horizontal in situ stress with be a factor of 3–5 smaller than the vertical stress for extension, the maximum magnitude of in situ stress at 5–10 km depth would be $\sigma_v = 62$–125 MPa. Because these values are on the same order as the impact-related stresses at the location of Pantheon Fossae, a corresponding radial increase of suitable magnitude caused by pre-existing uplift or some other mechanism would be required for the Pantheon Fossae to be explained by a combination of the Apollodorus impact in a stressed basin floor.

Our identification of two sequential cross-cutting sets of graben suggest a different multi-stage history for Pantheon Fossae. In addition, graben of set 1 were found to have significantly shallower depths of faulting than graben of set 2. The complexity of graben characteristics (Fig. 1b) and their different depths of faulting may be difficult to explain in the short time span implied between the Apollodorus impact and the deposition of its ejecta blanket.

4.2. Graben as surface expressions of dikes at depth

Graben at a planetary surface may be expressions of dikes at depth due to extensional stresses caused by the dike displacement (e.g. Rubin, 1992, 1995). These graben show a typical topographic signature that depends upon the depth of the dike below the surface and the magnitude of its opening displacement (e.g. Pollard, 1987; Delaney et al., 1987; Mastin and Pollard, 1988; Rubin and Pollard, 1988; Parker et al., 1990; Schultz et al., 2004). Even without topographic information, as used on Earth and Mars to quantitatively relate grabens to subsurface dikes, a comparison of calculated to predicted circumferential strain as well as comparisons to well-studied terrestrial and venusian radial dike complexes can be drawn.

Over-pressurized magma chambers compensate the pressure imbalances by fracturing the surrounding rock, forming steeply dipping radial dikes (e.g. Gudmundsson, 1988). These dikes then propagate radially outward from the magma chamber at shallow depths. Resultant circumferential strain can be predicted as a function of radial distance from the magma chamber. Following Johnson (1970), stresses exerted on the surrounding rock by the over-pressured magma chamber can be expressed in terms of their radial (σ_{rr}), circumferential ($\sigma_{\theta\theta}$), and shear ($\sigma_{r\theta}$) components in polar coordinates as:

$$\sigma_{rr} = p\left(\frac{r_0}{r}\right)^2, \tag{2}$$

$$\sigma_{\theta\theta} = -p\left(\frac{r_0}{r}\right)^2, \quad r \geqslant r_0, \tag{3}$$

and

$$\sigma_{r\theta} = 0, \tag{4}$$

where p is the magma pressure, r_0 is the radius of the magma reservoir and r is the radial distance away from the reservoir. In these equations, compressional stress and contractional strain are taken to be positive, while tensile stress and extensional strain are negative. In the text and figures, we discuss extensional circumferential strains as positive values. Strain in the circumferential direction, $\varepsilon_{\theta\theta}$, which can be accommodated at the surface by radially oriented graben, can be computed with Hooke's law in polar coordinates (Ugural, 1999):

$$\varepsilon_\theta = \frac{1}{E}(\sigma_\theta - v\sigma_r), \tag{5}$$

where v is Poisson's ratio and E is Young's modulus. A value of 0.25 was used for Poisson's ratio. Combining Eqs. (2) and (3) with Eq. (5) yields:

$$\varepsilon_\theta = \frac{p}{E}\left(\frac{r_0}{r}\right)^2(-1 - v). \tag{6}$$

Eq. (6) allows the computation of circumferential strain at the planetary surface as a function of radial distance from a magma reservoir. Like the dependence of impact shock waves and seismic waves, as explored in the previous section, the magnitudes of stresses generated from a magma reservoir are proportional to the inverse squared distance ($1/r^2$) away from the magma chamber. To compare predicted strains with strains calculated for Pantheon Fossae graben, the center of the six concentric traverses was shifted to the true projected center of convergence of the graben (white cross in Fig. 3) and values for total circumferential strain were calculated along them again. Results are comparable to the circumferential strain calculations from the previous analysis with values between ~2% and ~3.5%, strain values of >3% were observed along traverses 2–5 and lower values at traverses one and six at <3%. Calculated circumferential strain is shown in comparison to circumferential strain predicted around magma chambers of possible reservoir sizes of r_0 = 40 km and r_0 = 60 km, corresponding to the upper and lower limits of the innermost radial extents of Pantheon Fossae graben (with uncertainties related to cover by the Apollodorus crater ejecta blanket). Magma pressures and Young's modulus have units in MPa and are therefore taken as a ratio. Magma pressure is expected to have numeric values 1–2 orders of magnitude less than Young's modulus, resulting in plausible ratios of 0.1 and 0.01 (Fig. 5). As can be seen by inspection of Fig. 5, none of these curves of predicted circumferential strain match the calculated circumferential strain results for Pantheon Fossae, since the curves display a monotonic decrease of strain versus a relatively constant strain of 2–3% at the inner 120 km of Pantheon Fossae.

Pantheon Fossae graben have been suggested to be the surface expression of radial dikes at depth primarily because of their morphologic or geometric similarity to radial fracture complexes on Earth and Venus (e.g. Head et al., 2009). We statistically compare structures that are known or inferred to have formed in association with subsurface magma chambers to Pantheon Fossae graben in terms of their number of dikes or associated graben with distance from the center of the complex. The number of radial dikes emanating from magma chambers was counted for this paper along several circular traverses around magma chambers from terrestrial and inferred venusian radial dike complexes. Terrestrial radial dike swarms include Summer Coon Volcano, Colorado (Poland et al., 2008), Mauna Loa, Hawaii (Lockwood and Lipman, 1987), and Dike Mountain, Colorado (Johnson, 1970). Radial structures were counted around the example of the venusian nova given by Head et al. (2009). Venusian novae are inferred to be partly the result of dike emplacement at depth (Grosfils and Head, 1994). The terrestrial and venusian radial complexes show a consistent decrease in number of dikes with increasing distance from their origin (Fig. 6). However, the graben of Pantheon Fossae show a peaked frequency distribution, paralleling the radial circumferential strain distribution, where most graben are observed in the outer third of

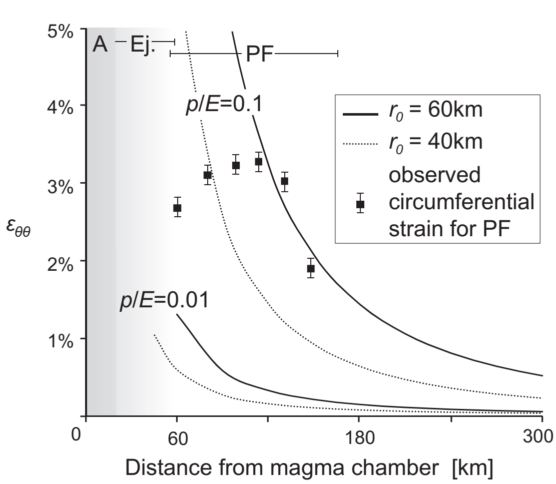

Fig. 5. Predicted circumferential strain decrease with distance away from magma chambers of sizes r_0 = 40 km and r_0 = 60 km are shown in relation to observed circumferential strain. Apollodorus (A), the extent of ejecta cover (Ej.) and the extent of graben at Pantheon Fossae (PF) are shown.

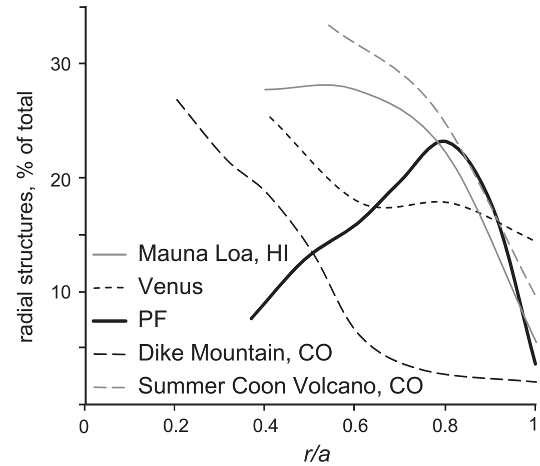

Fig. 6. Calculated percentages of total radial structures around a magma reservoir plotted against normalized distance away from the magma source for radial dikes and grabens on Earth and Venus. Distances from magma chamber (r) are normalized over the maximum extent of measured structures (a). Data sources given in text.

the main graben complex. Our investigation shows a marked discrepancy of the distribution of radial structures between Pantheon Fossae and confirmed terrestrial or inferred venusian radial dike swarms, implying that Pantheon Fossae is geometrically, and probably mechanically, different than radial dike swarms. This analysis of dike related graben also confirms the prediction of the magma chamber strain calculations (Fig. 5) of radially decreasing circumferential strains. Both analyses yield results that hinder the radial dike hypothesis for Pantheon Fossae graben.

Head et al. (2009) argued that echelon patterns of dikes (Fig. 1c) represent rotations of dikes to accommodate shallow near surface stress fields, following previous work such as Pollard et al. (1982). However, left and right step-over geometries at neighboring graben are both frequently observed at Pantheon Fossae (Fig. 1c). This pattern is inconsistent with the stress-rotation notion since two different near surface stress fields present at the same time would be necessary for the formation of echelon geometries of opposite senses (see Fink, 1985). Moreover, their study considers periodic buffered dike emplacement, due to an anomalous large magma supply, when referring to the few graben that extend >500 km to the outer Caloris basin. The amount of magma pressure necessary to form dikes of this length, however, would cause higher than observed circumferential strains closer to the magma chamber.

For decreasing magma pressures with increasing radial distance one would expect the widths of individual dikes to decrease along their lengths, leading to corresponding decreases in graben width and circumferential strain that are not observed (Figs. 1 and 5). The geometrical and cross-cutting relationships between the two graben sets would imply multiple episodes of dike injection at different depths. Constant depths of faulting, especially of the earlier and shallower grabens of set 1, argue against the radial dike hypothesis unless the magma chamber were quite small, so that the evidence for ascending dikes, recorded as radially narrowing and deepening graben (e.g. Rubin, 1992), would be covered by the Apollodorus crater and ejecta blanket. Our results collectively indicate that the graben of Pantheon Fossae are most likely not associated with dikes propagating outward from a shallow magma chamber at the center of the Caloris basin.

4.3. Mechanics of lithospheric doming

The radial extensional deformation observed at Pantheon Fossae has also been suggested to be the result of Caloris basin-interior uplift alone (Murchie et al., 2008; Watters et al., 2009b). Due to the axisymmetrical graben pattern, we consider axisymmetric vertical deflection of a circular plate as a mechanical model for doming of the Caloris floor (e.g. Gundmundsson, 1999) in order to quantitatively evaluate the magnitude of circumferential strain predicted by this model. Strains predicted by this model are then compared to the strain values obtained in this paper for Pantheon Fossae.

Radial (σ_r) and circumferential (σ_θ) stress components associated with axisymmetric deflection of a circular plate are given in polar coordinates by (Ugural, 1999):

$$\sigma_r = -\frac{3pz}{4d^3}[(1+v)a^2 - (3+v)r^2] \tag{7}$$

and

$$\sigma_\theta = -\frac{3pz}{4d^3}[(1+v)a^2 - (1+3v)r^2] \tag{8}$$

where p is the radially uniform vertical loading, d is the effective elastic thickness of the Caloris floor lithosphere, z is the vertical coordinate relative to the neutral plane in the middle of the plate (i.e. $z = 0$ at $d/2$) and r is the radial distance from the center, varying between 0 and a, with a being the total radius of the flexural uplift. For these conditions the vertical displacement is given by (Gundmundsson, 1999):

$$w = \frac{p}{64D}(a^2 - r^2)^2, \tag{9}$$

where D represents the flexural rigidity of the plate, which is given by Pollard and Johnson (1973) as

$$D = \frac{Ed^3}{12(1-v^2)}. \tag{10}$$

Circumferential strain can then be computed by substituting Eqs. (7) and (8) into Eq. (5). As in the previous section, compressional stress and contractional strain are taken to be positive, while tensile stress and extensional strain are negative; we refer in this section to circumferential extensional strain as positive numbers in the text and figures. The use of these equations limits the influence on strain to only three variables: the vertical component, z, which is related to the effective elastic plate thickness d; the uplift, w; and the total radius of the flexural uplift, a. For our analysis (Fig. 7), we have chosen a wide range of plausible plate thicknesses, uplift magnitudes, and plate radii in order to fully explore the range of variable space. Results are presented here for an area slightly larger than the radial extent of Pantheon Fossae, with $a = 300$ km (Fig. 7a), and for an area approximating the full radius of the Caloris basin, $a = 750$ km (Fig. 7b). Values of uplift magnitude at the plate center illustrated here are 5 km and 10 km, varying z (as function of $d/2$) to be 25 km, 50 km, and 75 km.

Results show that a Caloris basin-sized dome does not match the strain observations (Fig. 7b), but a smaller-scale uplift (Fig. 7a) does achieve remarkably good fits between predicted and observed strains. The best fit considered herein requires a maximum uplift of 10 km with a lithospheric thickness of 150 km. A dome of these dimensions would have slopes of only 1.4° in the Pantheon Fossae region. These results preclude doming of the entire Caloris basin floor due to a constant vertical loading as an explanation for the Pantheon Fossae graben. However, a dome of smaller radial extent can generate circumferential strains having the approximate magnitude and gradient to match those of the graben. A reasonable fit between predicted and observed strains can be achieved for small-radii domes by trading off values of plate thickness and uplift magnitude. Values in the literature for lithospheric thicknesses are broadly consistent with the value of 150 km used in this study; for comparison McKinnon (1986) and Melosh and McKinnon (1988) estimated values between 75 and 125 km, Kennedy et al. (2008) use values between 50 and 200 km, and Freed et al. (2009) consider 100–200 km as appropriate.

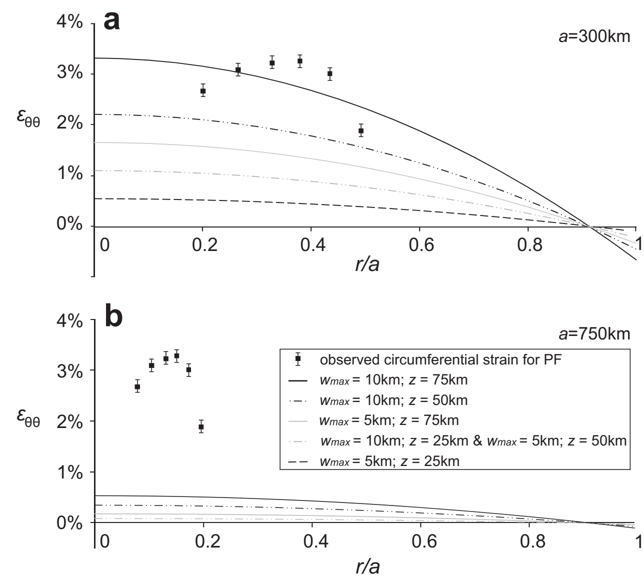

Fig. 7. Predicted circumferential strain from flexure of a lithospheric plate of different maximum uplifts w_{max}, and effective elastic thicknesses, compared to observed circumferential strain accommodated by Pantheon Fossae graben. (a) Strains predicted at the surface for a dome of radius $a = 300$ km for a series of maximum uplifts and elastic thicknesses. (b) Strains predicted for a dome of radius $a = 750$ km for the same series of maximum uplifts and elastic thicknesses.

Results for doming of the Caloris floor yield better fits to the observed data than the other formation hypotheses that we have evaluated, and suggest that doming may be the controlling factor for the formation of the radial graben. The doming hypothesis also generally agrees best with the observed graben pattern. The two observed graben sets can be explained by stress caused by the flexure of the lithosphere affecting different stratigraphic or mechanical units. Our results for uplift generally confirm results from the punctured-uplift model of Freed et al. (2009) and qualitatively confirm their theoretical predictions. Requirements to explain the extent and organized pattern of Pantheon Fossae therein also included significant amount of uplift, thick lithosphere and a symmetrical source of uplift.

As apparent in Eqs. (7) and (8), predicted radial and circumferential stresses in the very center of a axisymmetrical dome are equal. Resultant orientations of strain in the central area of uplift can therefore not be predicted at that one point. However, the model does not preclude that graben would form preferentially radial or circumferential patterns at some nonzero radial distance from basin center. Indeed, the calculations of Freed et al. (2009) predict unequal radial and circumferential stresses at small distances beyond the basin center. Given that topographic data for the Caloris basin are not yet available and given the simplicity of the mechanical model explored in this section, we chose not to investigate the trade space between uplift and the other parameters further in this paper. The analysis suggests however that the magnitude of circumferential strain accommodated by Pantheon Fossae graben can be used as a firm bound on current and future mechanical models of Caloris basin tectonics.

5. Conclusions and implications

We have qualitatively and quantitatively evaluated the three published origin hypotheses of Pantheon Fossae. Detailed observations and measurements from this study were used in order to assess the plausibility of the published hypotheses. Our observations at Pantheon Fossae provide a means to assess the predictions of current and future geodynamic models of Caloris tectonics.

An origin of the graben due to sudden stress changes triggered by the Apollodorus impact has been suggested (Freed et al., 2009), but our evaluation of the stress change distribution with distance from the crater (Fig. 4) does not support this hypothesis. Furthermore, results from our detailed mapping reveal that there are two different sets of graben distinguished by graben width, depth, and cross-cutting relationships. These graben characteristics, along with circumferential strain magnitudes calculated from the graben are also inconsistent with this hypothesis.

The structural expression and strain magnitudes of the observed graben array are difficult to achieve by the emplacement of radial dikes from a central magma reservoir. Head et al. (2008, 2009) described a series of graben characteristics as evidence for the graben of Pantheon Fossae to be surface expressions of dikes at depth. Our comparison of radial dike and graben systems from Earth and Venus to Pantheon Fossae reveal that Pantheon Fossae graben are not likely to be formed above dikes at depth. The existence of the two graben sets with different depths of faulting would further complicate this scenario. The fact that both graben sets occur in the same area with a similar radially varying strain distribution suggests, however, that they are likely to have formed from the same rather than two different, successive processes.

Lastly, we evaluated uplift of the Caloris basin floor for the formation of the graben of Pantheon Fossae. Murchie et al. (2008) and Watters et al. (2009b) both noted that Pantheon Fossae's radial graben in the central Caloris basin, which were unknown for pre-MESSENGER uplift models, contribute limiting conditions for new uplift studies. A mechanical model for lithospheric doming for the deflection of an axisymmetrical plate was used to examine the scale of a potential dome. Circumferential strains at the surface predicted by the uplift model best match our calculated strains for a dome somewhat larger in radial extent than Pantheon Fossae, with a radius of 300 km, a lithospheric thickness of 150 km, and a maximum uplift of 10 km. Yielding an acceptable match for the doming model not only shows that doming in the center of the Caloris basin is the likeliest of the evaluated hypotheses, but also supports the use of strain magnitudes accommodated by structures, such as the Pantheon Fossae graben, instead of computed stress magnitudes as in previous investigations, in providing bounds on models of Caloris basin tectonics.

Acknowledgments

We thank Chris Okubo for his help in creating the image mosaic used in this study and Tom Watters for help in determining image geometry data needed for the shadow length calculations. We thank the guest editor and two anonymous reviewers for their helpful comments that improved the quality of the manuscript. This work was supported in part by NASA's Planetary Geology and Geophysics Program.

References

Ahrens, T.J., O'Keefe, J.D., 1977. Equations of state and impact-induced shock-wave attenuation on the Moon. In: Roddy, D.J., Pepin, R.O., Merrill, R.B. (Eds.), Impact and Explosion Cratering. Pergamon Press, New York, pp. 639–656.

Byerlee, J.D., 1978. Friction of rocks. Pure Appl. Geophys. 116, 615–626.

Delaney, P.T., 1987. Heat transfer during emplacement and cooling of mafic dykes. In: Halls, H.C., Fahrig, W.F. (Eds.), Mafic Dyke Swarms. Geological Association of Canada, pp. 34–46.

Ernst, R.E., Grosfils, E.B., Mège, D., 2001. Giant dike swarms: Earth, Venus, and Mars. Annu. Rev. Earth Planet. Sci. 29, 489–534.

Fink, J.H., 1985. Geometry of silicic dikes beneath the Inyo Domes, California. J. Geophys. Res. 90, 11127–11133.

Freed, A.M., Solomon, S.C., Watters, T.R., Phillips, R.J., Zuber, M.T., 2009. Could Pantheon Fossae be the result of the Apollodorus crater-forming impact within the Caloris basin, Mercury? Earth Planet. Sci. Lett. 285, 320–327.

Grosfils, E.B., Head, J.W., 1994. The global distribution of giant radiating dike swarms on Venus: Implications for the global stress state. Geophys. Res. Lett. 21, 701–704.

Gudmundsson, A., 1988. Effect of tensile stress concentration around magma chambers on intrusion and extrusion frequencies. J. Volcanol. Geotherm. Res. 35, 179–194.

Gundmundsson, A., 1999. Postglacial crustal doming, stresses and fracture formation with application to Norway. Tectonophysics 307, 407–419.

Head, J.W., and 10 colleagues, 2008. Volcanism on Mercury: Evidence from the first MESSENGER flyby. Science 321, 69–72.

Head, J.W., and 12 colleagues, 2009. Evidence for intrusive activity on Mercury from the first MESSENGER flyby. Earth Planet. Sci. Lett. 285, 251–262.

Jaeger, J.C., Cook, N.G.W., 1979. Fundamentals of Rock Mechanics. Chapman and Hall, New York, p. 593.

Johnson, A.M., 1970. Dike patterns at Spanish Peaks, Colorado. In: Physical Processes in Geology. Freeman, Cooper, & Company, San Francisco, pp. 401–428.

Kennedy, P.J., Freed, A.M., Solomon, S.C., 2008. Mechanisms of faulting in and around Caloris basin, Mercury. J. Geophys. Res. 113, E08004. doi:10.1020/2007JE002992.

Krantz, R.W., 1989. Orthorhombic fault patterns: The odd axis model and slip vector orientations. Tectonics 8, 483–495.

Lockwood, J.P., Lipman, P.W., 1987. Holocene eruptive history of Mauna Loa Volcano. In: Decker, R.W., Wright, T.L., Stauffer, P.H. (Eds.), Volcanism in Hawaii, US Geological Survey Professional Paper 1350, pp. 509–535.

Mastin, L.G., Pollard, D.D., 1988. Surface deformation and shallow dike intrusion processes at Inyo Craters, Long Valley, California. J. Geophys. Res. 93, 13221–13235.

McKinnon, W.B., 1986. Tectonics of the Caloris Basin, Mercury. Paper Presented at the Mercury Conference, Div. Planet. Sci. Am. Astron. Soc. Intl. Astron. Union Comm. 16, Yuscon, Ariz., 6–9 August.

Melosh, H.J., 1989. Cratering mechanics: Excavation stage. In: Impact Cratering: A Geologic Process. Oxford University Press, New York, pp. 60–86.

Melosh, H.J., McKinnon, W.B., 1988. The tectonics of Mercury. In: Vilas, F., Chapman, C.R., Matthews, M.S. (Eds.), Mercury. The University of Arizona Press, Tuscon, pp. 374–400.

Murchie, S.L., and 10 colleagues, 2008. Geology of the Caloris Basin, Mercury: A view from MESSENGER. Science 321, 73–76.

Nicol, A., Watterson, J., Walsh, J.J., Childs, C., 1996. The shapes, major axis orientations and displacement patterns of fault surfaces. J. Struct. Geol. 18, 235–248.

Parker, A.J., Rickwood, P.C., Tucker, D.H. (Eds.), 1990. Mafic Dykes and Emplacement Mechanisms. Balkema, Rotterdam. 41pp.

Peacock, D.C.P., 2002. Propagation, interaction and linkage in normal fault systems. Earth-Sci. Rev. 58, 121–142.

Peacock, D.C.P., Sanderson, D.J., 1991. Displacement, segment linkage and relay ramps in normal fault zones. J. Struct. Geol. 13, 721–733.

Poland, M.P., Moats, W.P., Fink, J.H., 2008. A model for radial dike emplacement in composite cones based on observations from Summer Coon volcano, Colorado, USA. Bull. Volcanol. 70, 861–875.

Polit, A.T., Schultz, R.A., Soliva, R., 2009. Geometry, displacement-length scaling, and strain of normal faults on Mars with inferences on mechanical stratigraphy of the martian crust. J. Struct. Geol. 31, 662–673.

Pollard, D.D., 1987. Elementary fracture mechanics applied to the structural interpretation of dykes. In: Halls, H.C., Fahrig, W.F. (Eds.), Mafic Dyke Swarms Halls. Geological Association of Canada, pp. 5–24.

Pollard, D.D., Johnson, A.M., 1973. Mechanics of growth of some laccolithic intrusions in the Henry Mountains, Utah II: Bending and failure of overburden layers and sill formation. Tectonophysics 18, 311–354.

Pollard, D.D., Segall, P., Delaney, P.T., 1982. Formation and interpretation of dilatant echelon cracks. Geol. Soc. Am. Bull. 93, 1291–1303.

Rinehart, J.S., 1968. Intense destructive stresses resulting from stress wave interactions. In: French, B.M., Short, N.M. (Eds.), Shock Metamorphism of Natural Materials. Mono Book Corp., Baltimore, Maryland, pp. 31–42.

Rubin, A.M., 1992. Dike-induced faulting and graben subsidence in volcanic rift zones. J. Geophys. Res. 97, 1839–1858.

Rubin, A.M., 1995. Propagation of magma filled cracks. Annu. Rev. Earth Planet. Sci. 23, 287–336.

Rubin, A.M., Pollard, D.D., 1988. Dike-induced faulting in rift zones of Iceland and Afar. Geology 16, 413–417.

Scholz, C.H., 2002. The Mechanics of Earthquakes and Faulting, second ed. Cambridge University Press, New York.

Schultz, R.A., 1995. Limits on strength and deformation properties of jointed basaltic rock masses. Rock Mech. Rock Eng. 28, 1–15.

Schultz, R.A., Okubo, C.H., Goudy, C.L., Wilkins, S.J., 2004. Igneous dikes on Mars revealed by MOLA topography. Geology 32, 889–892.

Schultz, R.A., Moore, J.M., Grosfils, E.B., Tanaka, K.L., Mége, D., 2007. The Canyonlands model for planetary grabens: Revised physical basis and implications. In: Chapman, M. (Ed.), The Geology of Mars: Evidence from Earth-based Analogs. Cambridge University Press, New York, pp. 371–399.

Ugural, A.C., 1999. Uniformly loaded circular plates. In: Stresses in Plates and Shells, second ed. WCB McGraw-Hill, Boston, pp. 112–115.

Watters, T.R., Nimmo, F., 2009. The tectonics of Mercury. In: Watters, T.R., Schultz, R.A. (Eds.), Planetary Tectonics. Cambridge University Press, Cambridge, pp. 15–80.

Watters, T.R., Nimmo, F., Robinson, M.S., 2005. Extensional troughs in the Caloris Basin of Mercury: Evidence of lateral crustal flow. Geology 33, 669–672.

Watters, T.R., Solomon, S.C., Robinson, M.S., Head, J.W., André, S.L., Hauck II, S.A., Murchie, S.M., 2009a. The tectonics of Mercury: The view after MESSENGER's first flyby. Earth Planet. Sci. Lett. 285, 283–296.

Watters, T.R., Murchie, S.L., Robinson, M.S., Solomon, S.C., Denevi, B.W., André, S.L., Head, J.W., 2009b. Emplacement and tectonic deformation of smooth plains in the Caloris basin, Mercury. Earth Planet. Sci. Lett. 285, 309–319.